Journal of Sustainable Development; Vol. 7, No. 1; 2014
ISSN 1913-9063 E-ISSN 1913-9071
Published by Canadian Center of Science and Education

Thermal Performance Improvement of Derna Electric Power Station (unit5) Using Solar Energy

Yasser Aldali[1] & K. Morad[1,2]

[1] Faculty of Engineering, Mechanical Engineering Department,Omar Almokhtar University, Derna, Libya

[2] Faculty of Engineering, Port Said University, Egypt

Correspondence: Yasser Aldali, Mechanical Engineering Department, Omar Al Mokhtar University, Derna, Libya. E-mail: y.aldali@napier.ac.uk

Received: November 12, 2013 Accepted: December 28, 2013 Online Published: January 8, 2014

doi:10.5539/jsd.v7n1p60 URL: http://dx.doi.org/10.5539/jsd.v7n1p60

Abstract

The use of fossil fuels should be reduced in near future due to their limited resources and increasing ecological impacts. Therefore, increased interest and incentives have been created for developing electricity supply utilizing renewable energy such as solar energy, which has long-range potential and is applicable in most geographical regions. The objective of this paper is to perform thermodynamic and economic analysis of the proposed integrated solar Derna steam turbine power plant (unit 5) based on the parabolic trough system. Two modes of operation are considered: power boosting mode in which solar energy is used to preheat the feed water in the low and high-pressure preheaters and fuel saving mode in which a fraction of saturated steam is generated by the solar collector field. A simulation mathematical model has been developed for each component of the plant. Also different thermodynamic performance parameters at all points of the plant are considered in the calculations. This study shows that the maximum increasing of overall efficiency of the integrated solar steam power plant (ISSPP) are 5.9% for fuel saving mode and 3.2% for power boosting mode for 21st July at 12:00 with DNI 810 W/m^2. During 25 years operating period of solar field, the fuel saving mode saves approximately 121 million $ and reduces about 125,000 ton in fuel consumption and approximately 390,000 ton in CO_2 emissions while the augmentations of electrical energy for the power boosting mode are about 360,879 MWh. The study also shows that the paybacks of the solar field cost for the power boosting and fuel saving modes of operation are approximately 15.7 and 11.5 years, respectively.

Keywords: integrated solar steam power plant, thermodynamic and economic analysis, concentration solar power, parabolic trough collectors, fuel saving mode, power boosting mode

Nomenclatures

AF	air to fuel ratio, kg/kg$_{fuel}$	C	fraction of carbon in oil fuel, kg/kg$_{fuel}$
h	enthalpy, kJ/kg	C_p	specific heat at constant pressure, kJ/kg.^{o}C
m	mass fraction	Hu	lower heating value of oil fuel, kJ/kg
$\dot{m}$	mass flow rate, kg/s	H	fraction of hydrogen in oil fuel, kg/kg$_{fuel}$
M	molecular weight, kg/kmol	N	fraction of nitrogen in oil fuel, kg/kg$_{fuel}$
n	mol fraction, kmol/kmol	O	fraction of oxygen in oil fuel, kg/kg$_{fuel}$
P	pressure, bar	S	fraction of sulfur in oil fuel, kg/kg$_{fuel}$
T	temperature, ^{o}C	DT	temperature difference, ^{o}C
w	specific work, kJ/kg		

Greeks

η	efficiency	ϕ	relative humidity of moist air
λ	excess air factor		

Subscripts

B	boiler	th	theoretical

s	steam	*sol*	solar steam
G	combustion gases	*R*	reaction
P	pump	*pp*	pinch point
T	Turbine	*f*	saturated water
g	saturated vapor	*fg*	difference between saturated liquid and vapor
w	water at boiler inlet		

Abbreviations

DSG	direct steam generation	LEC	Levelized Electricity/Energy Cost
ISFPP	integrated solar-fossil power plants	PT	parabolic trough
SEGS	solar electric generating systems	ISSPP	Integrated Solar Steam Power Plant
O&M	Operational and Maintenance	CSP	Concentration Solar Power
PTS	Parabolic Trough System	IAPWS	International Association for the Properties of Water and Steam

1. Introduction

Electricity production using solar thermal energy is one of the main research areas at present in the field of renewable energies. With levelized electricity costs (LEC) of 0.10-0.12 $US/kWh the well-known SEGS (Solar Electric Generating Systems) plants in California are presently successful solar technology for electricity generation (Eck et al., 2003). The SEGS plants apply a two-circuit system, consisting of the collector circuit and the Rankin cycle of the power block. These two-circuits are connected via a heat exchanger. In the case of the Direct Steam Generation (DSG) in the collector field, the two-circuit system turns into a single-circuit system, where the collector field is directly coupled to the power block. This renders a lower investment and higher process temperatures resulting in higher system efficiency. Due to the lower investment and the higher efficiency a reduction of the LEC of 10% is expected when the DSG process is combined with improved components of the solar collectors (Valenzuela et al., 2006).

Eck et al. (2003) investigated a direct steam generation (DSG) solar thermal power plants. The paper investigated the advantages, disadvantages, and design considerations of a steam cycle operated with saturated steam for the first time. Two types of plants were analyzed and compared in detail: a power plant with synthetic oil and a DSG power plant. It is found that the LEC of a DSG plant could be higher than those of a synthetic oil plant. When considering a plant without solar thermal storage on the other hand, the DSG system could reduce the LEC. Garcia et al. (2011) paper describes a simulation model of parabolic trough solar thermal power plants with a thermal storage system. Model results for a 50 MWe power plant are presented and compared to real data from an equivalent power plant currently operated by the ACS Industrial Group in Spain. Garcia-Barberena et al. (2012) analyzed the influence of operational strategies on the performance of parabolic trough (PT) solar power plants with the aid of SimulCET a computer program for the simulation of the energy behavior of PT plants developed by the National Renewable Energy Centre of Spain. Comparing with experimental data it showed good agreement among daily averaged estimates and the corresponding measured energy values with mean deviation of ± 3.14%. Montes et al. (2009) presented an economic optimization of the solar multiple for a solar-only parabolic trough plant. Five parabolic trough plants have been considered, with the same parameters in the power block but different solar field sizes. Thermal performance for each solar power plant has been featured, both at nominal and part-load conditions. Once annual electric energy generation is known, LEC for each plant was calculated, yielding a minimum LEC value for a certain solar multiple values within the range considered. A mathematical model of 30-MW SEGS solar power plant was established by Abdel Dayem et al. (2013). Annual performance of the plant was presented under weather conditions of Makkah 21.4 °N. Direct steam generation plant was studied with higher power generated. The power was highly improved by about 45% along the year.

Solar energy is often available in abundant quantities in the vicinity of conventional steam or combined power plants, where the need for clean add-on power is substantial. Fossil-fuel based power units can be augmented with solar thermal power for feed water preheating or parallel steam generation.

Integrated Solar-Fossil Power Plants (ISFPP) represent, both economically and energetically, a promising alternative for the conversion of solar energy while offering a guarantee of a minimum power supply independent of the level of solar radiation (Wood, 2008; Torres et al., 2013; Khaldi, 2011; Peterseim et al., 2012).

Their performance is however strongly dependent on the intensity of the solar input. Taking account of the classical thermo-economic criteria (performances/costs), several integration concepts and technology options were used (Kelly et al., 2011; Horn et al., 2004; Hosseini et al., 2005).

It should be underlined that successful integration of solar thermal power into conventional steam plants relies on the availability of large patches of land adjacent to the plant and of course on a considerable solar insolation resource at the given location. This narrows the possible choices only to steam plants outside densely populated areas and also situated in the sun belt of the globe – generally at latitudes between 20 to 40 degrees north or south.

Libya, located in the Middle East and North Africa (MENA) region, is counted among the best insolated areas. Over the country land, estimated at 1.75 million km^2, the Sahara represents 86%. It is exposed daily to a direct sun irradiation of 8.1 kWh/m^2/day in southern region and 6 kWh/m^2/day in the coastal region (Elsaket, 2007). These solar potential and land resources are optimal for the implementation of ISFPP.

The main objective of the present study is carried out to simulate and analyze the performance of a proposed Integrated Solar Steam Power Plant (ISSPP) site in Derna city. Derna, which is a region located in Northern-East Libya has a solar energy potential ranging from 2000 to 2100 kWh/m^2/year of direct normal irradiation.

Two solar thermal hybrid steam integration modes are considered, namely:

- To aid with feed water preheating for the steam cycle, thus saving the extracted steam otherwise bled from the turbine for that purpose (Power boosting mode).
- To assist with parallel saturated steam generation at the necessary pressure level, while the solar-produced steam can further be superheated and expanded in the conventional steam cycle (Fuel saving mode).

2. Analysis of Integrated Solar Steam Power Plant

2.1 Solar Field

The main factor that affects the concentration solar power (CSP) plant size, performance and thus land occupation is the direct irradiation (beam irradiation).

In this paper, the monthly averaged global radiation on the horizontal plane was made available for Derna by the Libyan Meteorological Office. The Liu and Jordan (1960) model which describes the relationship between beam radiation and diffuse radiation particles provides a reliable method for estimating the radiation incident on any given surface on an hourly basis given the monthly-averaged figures for the global combination of these two components (Tham et al., 2010). Figure 1 describes the calculation scheme used.

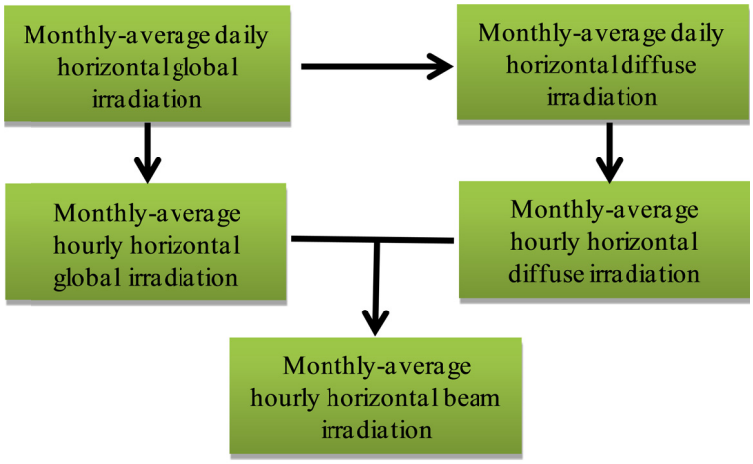

Figure 1. Calculation scheme for monthly-average hourly beam irradiation

The specifications of the parabolic trough collector PTC system are detailed in Table 1.

Table 1. Parabolic trough collector system specifications

Physical dimensions of collector construction		Reference
1. Inner diameter of absorber tube	50 mm	(Zarza et al., 2004)
2. Outer diameter of absorber tube	70 mm	(Zarza et al., 2004)
3. Inner diameter of glass cover	85 mm	(Zarza et al., 2004)
4. Outer diameter of glass cover	90 mm	(Zarza et al., 2004)
5. Aperture presented by one collector	5.76 m	(Zarza et al., 2004)
Physical characteristics of the materials used in the construction of the collectors		
6. Transmissivity of glass cover	0.85	(Sukhatme et al., 2008)
7. Emissivity of absorber tube	0.05	(Sukhatme et al., 2008)
8. Emissivity of glass cover	0.88	(Sukhatme et al., 2008)
9. Absorptivity of absorber tube	0.95	(Sukhatme et al., 2008)
Plant design parameters		
14. Mass flow rate of water/steam for one loop	0.8 kgs^{-1}	(Zarza et al., 2004)
17. Concentration ration PTC	25.87	

To harness the maximum amount of solar radiation, the orientation and tracking of a Parabolic Trough System (PTS) is of paramount importance. A PTS is oriented with its focal axis pointed either in the east-west (E-W) or north-south (N-S) direction. In the E-W orientation, the focal axis is horizontal, while in the N-S orientation, the focal axis may be horizontal or inclined. According to Aldali et al. (2011) five modes of parabolic trough collectors can be used according to their orientation and sun tracking capabilities.

Five different modes of tracking are discussed herein.

- Mode 1 offers a horizontal focal axis along the east-west plane. The collector is rotated about a horizontal east–west axis with a daily adjustment required to ensure that noon beam irradiation is normal to the collector aperture.
- Mode 2 is similar to mode 1, but with a continuous adjustment of the collector such that the beam irradiation is incident on the collector aperture with a minimum angle throughout the day.
- Mode 3 is similar to mode 2, but with a horizontal focal axis along the north–south plane.
- Mode 4 is similar to mode 3, but with the focal axis being at a fixed inclination that is equal to the latitude of the location. The collector is rotated about an axis parallel to earth's axis at an angular velocity that is equal and opposite to the earth's rotational rate.
- Mode 5 is similar to mode 4, but with the collector now subjected to a two-dimensional motion, i.e., the collector is rotated about the focal axis as well as about a horizontal axis perpendicular to this axis. The beam irradiation is thus always normal to the collector aperture.

In this study a substantial energy gain from mode 3 of operation as opposed to mode 2 and hence the former was selected for the present design study.

2.2 Steam Power Plant

The Derna steam power plant, as shown in Figure 2, consists of a single pressure boiler, 65MW steam turbine, a condenser, a condensate pump, a low-pressure feed water heater, a deaerator, a feed water pump, and a high-pressure feed water heater. The design parameters are listed in Table 2. The pinch point temperature difference of 15 °C is considered and a design stack temperature of 130 °C was selected which is higher than the dew point temperature (125 °C) of the combustion product.

Table 2. Design parameters of Derna steam power plant

proximate analysis of oil Fuel	85.2% C, 11% H_2, 2.4% O_2, 1.15% N_2 and 0.25% S
Ambient air conditions	25 ^oC, 1 bar, 60% relative humidity
Live steam conditions	87 bar and 550 ^oC, 66.815 kg/s
Pressure of extracted steam for HP feedwater heater	21.8 bar
Deaerator pressure	6.02 bar
Pressure of extracted steam for LP feedwater heater	1.15 bar
Condenser pressure	0.062 bar
Steam turbine adiabatic efficiency, η_T	85%
Pump polytropic efficiency, η_p	75%
Mechanical efficiency, η_m	97%
Generator efficiency, η_G	98%
Boiler efficiency, η_c	98.5%

2.3 Modes of Operation

For the integrated solar steam cycle, the solar field should not complicate any operation. Moreover, the operation of steam cycle plant should not be affected due to the integration to the solar field. From these design targets of the solar supported plant, there are two different operating modes: power booster mode and fuel saving mode. During cloudy periods or at night, the integrated plant operates as a conventional steam cycle facility.

In fact, both the power boost and the fuel saving modes are applicable in real conditions. Most modern steam cycles are able to handle increased steam mass flows (boosted power output) with up to around 10% above the rated turbine capacity, and this scenario is very suitable for augmented power generation during peak sunshine hours to cover the peak consumption for air conditioning. On the other hand, fuel saving mode is very relevant to reducing the use of fossil fuel, therefore reducing the emissions of any related pollutants and improving the environmental footprint of existing steam plants, while the steam boiler usually improves its thermal efficiency when operated at loads lower than the nominal one (Popov, 2011).

A schematic diagram of the power booster mode is shown in Figure 2. Steam that is extracted from the turbine to provide feed water preheating is now allowed to expand in the turbine, while the preheating loads for both low- and high-pressure heaters are instead covered by the solar field. The steam turbine in power booster mode is rated larger than those for a fossil only operated steam cycle.

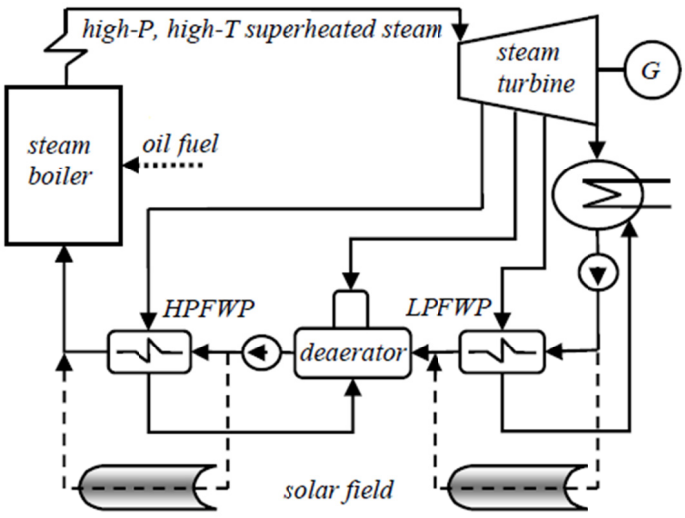

Figure 2. Power booster mode of operation for ISSPP

By the fuel saving mode of operation (Figure 3), the integration is achieved by boiling a fraction of the feed-water equivalent to the amount of steam extracted for both low- and high-pressure heaters in the solar boiler and feeding saturated high-pressure steam into the steam cycle at the inlet to the superheater in the boiler. The most efficient use of solar thermal energy is the production of high pressure saturated steam. During sunny periods feed water is withdrawn from the steam cycle Plant at boiler inlet and converted to saturated steam in the solar steam generator. The saturated steam is returned to the boiler, and the combined fossil and solar steam flows are superheated in the boiler. During cloudy periods or at night, the integrated plant operates as a conventional combined cycle facility. This means that the fossil firing will be reduced as a result of solar steam generation.

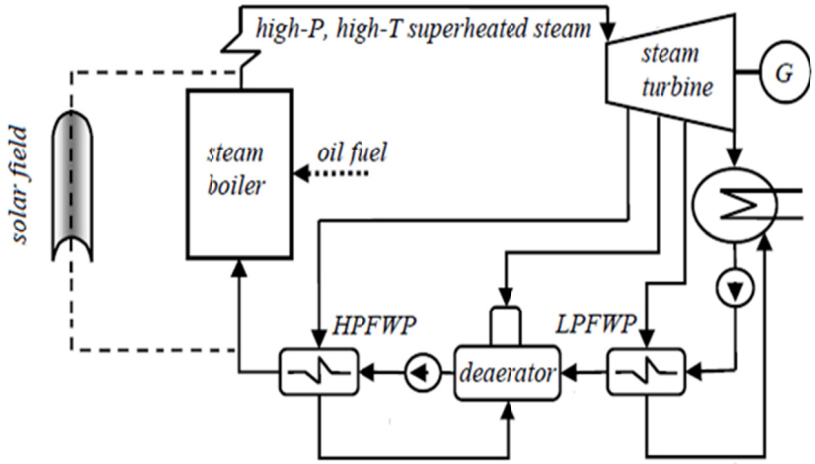

Figure 3. Fuel saving mode of operation for ISSPP

3. Mathematical Modeling

For the purpose of analysis it is assumed that: The ISSPP operates at a steady state. Each component of the ISSPP is treated separately and their models are developed in detail in the following sections.

3.1 Solar Concentrator Field

Aldali et al. (2011) developed and presented models and calculations of the result implementations of the 2007 revision of the International Association for the Properties of Water and Steam (IAPWS) equations in a general application based on Microsoft Excel and VBA.

According to Aldali et al. (2011), the aim of the model is to describe the thermodynamic and thermophysical properties of the water and steam which act as the heat transfer vector. Using the results from the model, other practical calculations can be performed, such as establishing the length of absorber tube capable of delivering the design collectors loop through solar energy alone during periods of peak insolation, and calculating the oil requirement to maintain the design capacity at other times.

In this study, the authors have used the mentioned model to calculate thermodynamic and thermophysical properties, oil usage, and solar fraction for the solar concentrator field.

3.2 Steam Turbine Cycle

The performance of the steam cycle plant is calculated based on the designed mass flow rate of generated steam from the boiler, $\dot{m}_s$, of 66.815 kg/s, pinch point temperature difference (ΔT_{PP} as shown in Figure 4) of 15 °C, and stack temperature ($T_{g,out}$) of 130 °C. The mass flow rate of the combustion gases is calculated by applying energy balance for the superheating and evaporating sections of the boiler.

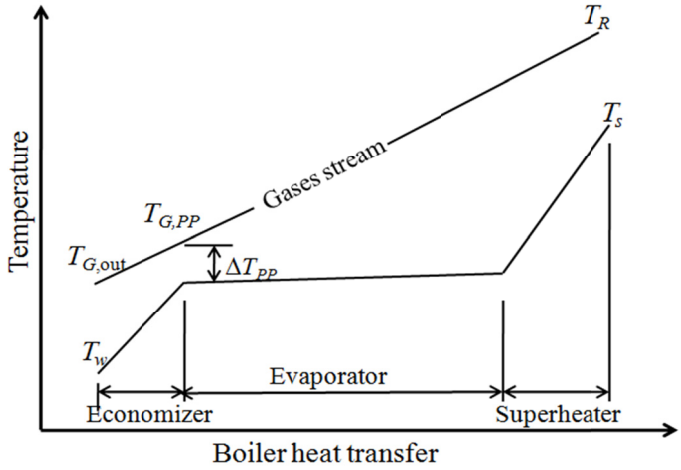

Figure 3. Boiler heat transfer diagram

$$\dot{m}_G = \frac{(\dot{m}_s - \dot{m}_{sol}).h_{fg}(P_B) + \dot{m}_s.[h_s - h_g(P_B)]}{C_{p,G}.(T_R - T_{G,pp})} \quad (1)$$

The energy balance equation for the economizer section

$$\dot{m}_G C_{p,G}.(T_{G,pp} - T_{G,out}) = (\dot{m}_s - \dot{m}_{sol})(h_f(P_B) - h_w) \quad (2)$$

where $\dot{m}_{sol}$ is the solar steam flow rate ($\dot{m}_{sol}$ = 0 for conventional steam turbine cycle and power booster mode).

The reaction temperature of the combustion process of the fuel oil is calculated by applying mass and energy balance as follows

$$\dot{m}_G = \dot{m}_F.(AF + 1) \quad (3)$$

$$T_R = \frac{\eta_{c.c} Hu + AF.C_{p,air}.T_{air}}{(AF + 1).C_{p,G}} \quad (4)$$

Theoretical number of air kmol required per kg of fuel

$$nair,th = (mC/MC + 0.5.mH/MH + mS/MS + mN/MN - mO/MO)/0.21 \quad (5)$$

The air to fuel ratio, *AF*, is calculated as follows

$$AF = n_{air,th}.\ \lambda.M_{air} \quad (6)$$

The mole fraction of water vapor in combustion moist air is

$$n_{H_2O} = \frac{\phi.P_{sat}(T_{air})}{P_{air}} \quad (7)$$

The mass flow rate of emission of CO_2 is calculated as follows

$$\dot{m}_{CO_2} = \dot{m}_G \cdot \frac{m_C}{m_C / M_C + 0.79..\lambda.n_{air,th} + 0.21.(\lambda - 1)..n_{air,th} + m_H / M_H + n_{H_2O} + m_S / M_S} \cdot \frac{1}{M_G} \quad (8)$$

The net electrical power generated is calculated as follows

$$\dot{W}_{elec} = \dot{m}_s.(w_T.\eta_m - w_P / \eta_m).\eta_G \quad (9)$$

The overall efficiency of energy conversion based on the fuel consumption (energy that costs) is calculated as follows:

$$\eta_{overall} = \frac{\dot{W}_{elec}}{\dot{m}_F.Hu} \quad (10)$$

A computer program was developed based on Fortran language to solve the set of equations by assuming initial guess value of excess air factor, λ, and calculated the stack gas temperature, $T_{g,out}$, and compare the calculated

$T_{g,out}$ with the fixed value of stack gas temperature of 130 °C and repeat the calculations with assuming another value of λ unit the calculated $T_{g,out}$ approaches the value of 130 °C.

4. Full Load Results

Table 3 displays the power generation, oil fuel consumption, overall efficiency of energy conversion, and the mass flow rate of CO_2 emissions for the two considered modes of operation at full load compared to the conventional steam cycle plant. The results are given for 21st March with DNI 490 W/m^2, 21st July with DNI 810 W/m^2, and 21st December with DNI 487 W/m^2 at 12:00. As indicated in Table 2, for 21st July, the fuel saving mode results in reduction of fuel consumption and emission of CO_2 by approximately 15.3% and increasing in overall efficiency of approximately 5.9%, while the power booster mode results in increasing of electrical power by about 9.7% and 3.2% increasing in overall efficiency compared to the conventional steam cycle operating at full load. For 21st March, the fuel saving mode results in reduction of fuel consumption and CO_2 emission by approximately 8.6% and increasing in overall efficiency by approximately 3.1%, while the power booster mode results in improvement of electrical power by approximately 6% and 1.2% increasing in overall efficiency compared to the conventional steam cycle operating at full load. For 21st December, the fuel saving mode results in reduction of fuel consumption and CO_2 emission by approximately 2.3% and increasing in overall efficiency by approximately 0.9%, while the power booster mode results in improvement of electrical power by about 2.7% and 0.7% increasing in overall efficiency compared to the conventional steam cycle operating at full load.

Table 3. Output data for different modes of operation

Arrangement mmkjk;';/	$\dot{W}_{elec}$ (MW) (21st at 12:00)			$\dot{m}_{fuel}$ (kg/s) (21st at 12:00)			$\eta_{overall}$ (%) (21st at 12:00)			$\dot{m}_{CO_2}$ (kg/s) (21st at 12:00)		
	Mar.	Jul.	Dec.	Mar.	Jul.	Dec.	Mar.	Jul.	Dec.	Mar.	Jul.	Dec.
Booster mode	68.92	71.29	66.77	4.423	4.423	4.423	35.0	36.2	33.7	13.82	13.82	13.82
Fuel saving mode	65.0	65.0	65.0	4.044	3.745	4.322	36.1	38.9	33.9	12.64	11.70	13.50
Conventional plant	65.0	65.0	65.0	4.423	4.423	4.423	33.0	33.0	33.0	13.82	13.82	13.82

5. Economic and Environmental Benefits

For economic evaluation of the ISSPP, it is relevant to compare the cost of the solar field and resulted cost of fuel savings estimated in Table 3 together with the evaluated CO_2 reduction cost for the fuel saving mode or revenues for solar augmenting the capacity of producing electricity in the power plant for the power boosting mode. For doing the economic study we will assume that the steam turbine plant is already built and currently in operation and due to the development of the solar technologies we want to equip the present steam turbine cycle with a solar field for power boosting mode or fuel saving mode. The economic and environmental analysis was best determined by calculating the outputs of the ISSPP on an hourly basis, and summing the results over the course of a year. For simplicity, all of the annual performance calculation is based on 10 hours per day of usable sunlight during the whole year, and a 25 years collector lifetime.

5.1 Solar Field Costs

The collector surface area needed for reaching the amount of solar heat required are 38572.32 m^2 for power boosting mode and 77709.24 m^2 for fuel saving mode. The collector surface is the mirrored surface needed for absorbing the radiation, which is different from the total surface of the solar field. The rows of collector have to keep a distance between them because of the shading effects for low incident angles. This distance is approximated as three times the aperture of the collectors and it allows to determine the land surface necessary for installing the solar field. Assuming that the land use factor is 3.5, the total surface required for installing the solar field is:

$$A_{solar\ field} = A_{collector} \times 3.5 \qquad \text{m}^2 \tag{11}$$

For the study we assume estimated specific costs for the PTC technology of around 300 \$/m^2 (Da Rocha, 2010). By multiplying the collector price per square meter and the square meters of collector surface we can calculate the capital expenditure (CAPEX):

$$CAPEX = A_{collector} \times 300\ \$/\text{m}^2 \qquad \$ \tag{12}$$

That is the required initial investment for building the solar field at the beginning of the construction. But for paying the construction during the period of operation of the solar field we have to calculate the annuity. The annuities are the fixed payments which have to be done every year during the predicted life of operation of the solar field for payback of the initial investment. The annuity includes the price of the construction and the increase of interest rate every year. Considering a period of operation of 25 years (T) and an interest rate of 8% (r), the annuity is calculated as (Da Rocha, 2010):

$$a = \frac{(1+r)^T .r}{(1+r)^T - 1} \qquad \text{year}^{-1} \tag{13}$$

And the yearly payment is:

$$\text{Payment/year} = CAPEX \times a \qquad \$/\text{year} \tag{14}$$

which in 25 years makes a total of:

$$\text{Total Payment} = \text{Payment/year} \times 25 \qquad \$$$

The total payment for the solar field for power boosting mode is approximately 27.2 million $ and for fuel saving mode is approximately 54.8 million $.

5.2 Power Boosting Mode

Figure 4 shows the monthly augmentations of electrical energy. The largest augmentations of electrical energy are in July (approximately 2057 MWh) while the smallest augmentations of electrical energy are in January (approximately 376 MWh). The economic strategy based on solar augmented is dependent on the surplus that is being produced at the generator, that is, the capacity to boost the electricity production compared to the conventional steam power plant. The expected revenue $R_{\text{power boosting}}$ is calculated by multiplying the summation of the monthly augmentations of electrical energy, ΔW_{elec}, shown in Figure 4, to the electricity tariff T_{elec}.

$$R_{\text{power boosting}} = T_{elec} \times \sum_{\text{Jan}}^{\text{Dec}} \left[\left(\sum_{i=1}^{N} \Delta \dot{W}_{ekec,i} \right) \times \text{No. of day/month} \right] \quad \$/\text{year} \tag{15}$$

where N is the number of hours of usable sun per day (10 hours). With respect to T_{elec}, the average 2013 tariffs for the very high voltage production of electricity of T_{elec} = 120 $/MWh will be considered. The expected annual revenues for solar augmenting the capacity of producing electricity in the power plant are approximately $US3.87 million. During 25 years operating period of solar collectors, the power boosting mode increases the electrical energy produced by the steam power plant by approximately 360,879 MWh.

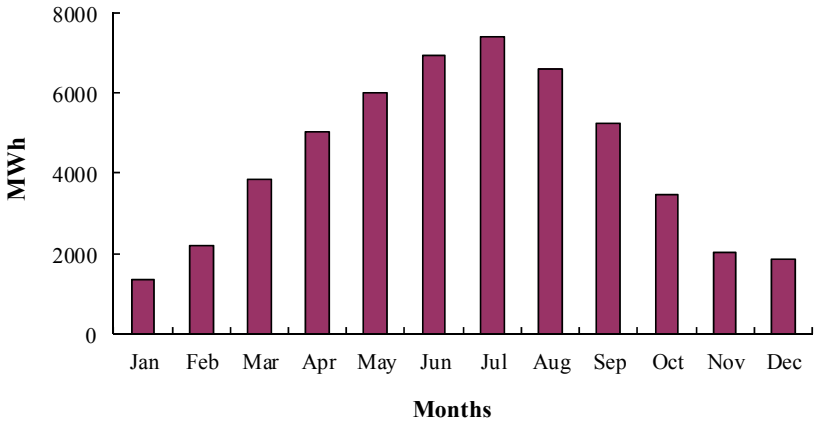

Figure 4. Monthly augmentations of electrical energy for power boosting mode

5.3 Fuel Saving Mode

Figure 5 shows the monthly reductions of the fuel consumptions and CO_2 emissions. The largest amount of fuel saving (approximately 685 ton) and CO_2 emissions (approximately 2141 ton) are in July while the smallest amount of fuel saving (approximately 165 ton) and CO_2 emissions (approximately 515 tons) are in January. Since the fuel saving mode requires less fuel than a conventional steam turbine cycle due to its fraction of steam

generated from the solar field, the operation of fuel saving mode reduces total CO_2 emissions. The avoided emissions can be set in relation to the incremental cost in order to calculate the avoidance costs in US$ per ton of CO_2 avoided. Therefore, economic strategy underlying the fuel saving mode is based on two different prices. Firstly, the national price of fuel oil, FS, concerns the fuel savings derived from the operation of reducing boiler's heat load. Secondly, C_{CO_2} the credit support due to equivalent CO_2 emissions avoidance shall be taken into account for the calculations. The sum of the two parameters will give the expected revenue using a fuel saving approach.

$$R_{\text{fuelsaving}} = \sum_{\text{Jan}}^{\text{Dec}} \left[\sum_{i=1}^{N} \left(m_{\text{fuel saved}j} \times FS + m_{\text{CO}_2\ \text{saved}j} \times C_{\text{CO}_2} \right) \times \text{No.of days/month} \right] \quad \$/\text{year} \tag{16}$$

where $m_{\text{fuel saved}}$ and $m_{\text{co2 saved}}$ are the reduction of the fuel consumption and CO_2 emissions per hour of usable sun. The FS in 2013 is approximately 935 \$/ton while the value of C_{CO_2} which is presently applied by the World Bank is approximately 11 US\$/ton (El-Sayed, 2005). Then the expected annual revenues for fuel saving mode are 4.84 million \$. During 25 years operating period of solar collectors, the fuel saving mode saves 121 million \$ and reduces approximately 125,000 ton in fuel consumption and 390,000 ton in CO_2 emissions.

Depending on above analysis, the paybacks for the power boosting and fuel saving modes of operation are approximately15.7 and 11.5 years, respectively.

As solar thermal energy is the cleanest renewable energy of zero emission, its utilization performs a reduction of greenhouse gas emission and meets with the policy of governments to promote measures against global warming. For fuel saving mode, the greenhouse gas (CO_2) emission is reduced by approximately 15600 tons/year in comparison with a conventional steam turbine power plant.

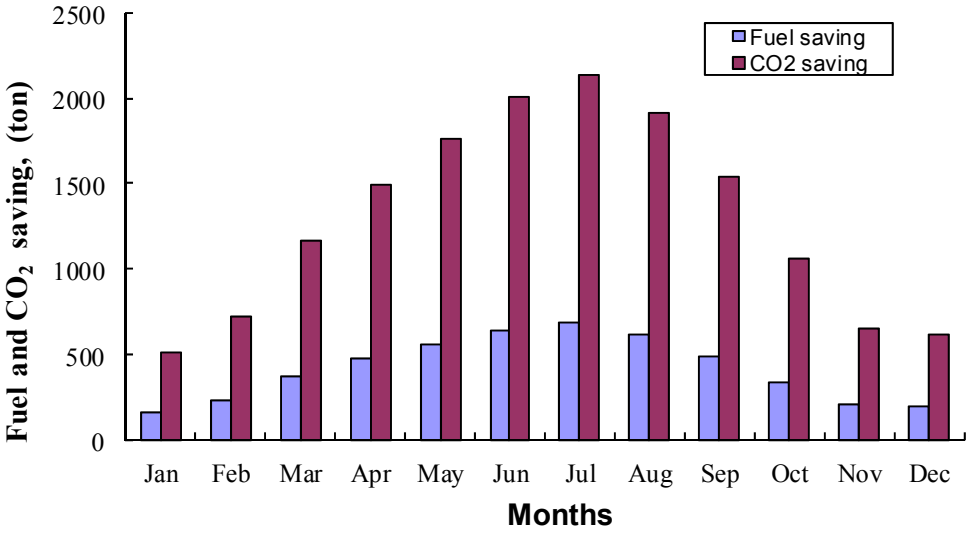

Figure 5. Monthly Fuel and CO_2 saving for fuel saving mode

6. Conclusions

An integrated solar steam power plant (ISSPP) was thermodynamically and economically studied. Both power boosting and fuel saving modes were considered in this study. The computer code developed enabled matching the solar collectors with the steam power plant. The main conclusions of this task are:

- For 21st July at 12:00, the fuel saving mode results in reduction of fuel consumption and emission of CO_2 by approximately 15.3% and increasing in overall efficiency of approximately 5.9%, while the power booster mode results in improvement of electrical power by about 9.7% and 3.2% increasing in overall efficiency compared to the conventional steam cycle operating at full load. For 21st December at 12:00, the fuel saving mode results in reduction of fuel consumption and CO_2 emission by approximately 2.3% and increasing in overall efficiency by approximately 0.9%, while the power booster mode results in improvement of electrical power by about 2.7% and 0.7% increasing in overall efficiency compared to the conventional steam cycle operating at full load.

- The collector surface area and total payment for the solar fields are approximately 38572 m^2 and US$ 27.2 million for power boosting mode and 77709 m^2 and US$ 54.8 million for fuel saving mode.
- For power boosting mode, largest augmentations of electrical energy are in July (approximately 2057 MWh) while the smallest augmentations of electrical energy are in January (approximately 376 MWh). For fuel saving mode, the largest amount of fuel saving and CO_2 emissions are in July (approximately 685 and 2141 tons, respectively) while the smallest amount of fuel saving and CO_2 emissions are in January (approximately 165 and 515 tons, respectively).
- During 25 years operating period of solar field, the fuel saving mode saves approximately US$ 121 million and reduces approximately 125,000 ton in fuel consumption and 390,000 ton in CO_2 emissions while the augmentations of electrical energy for the power boosting mode are approximately 360,879 MWh.
- The paybacks of the solar field cost for the power boosting and fuel saving modes of operation are approximately 15.7 and 11.5 years, respectively.

References

Abdel Dayem, Nabil Metwally, A. M., M., Alghamdi, A. S., & Marzouk, E. M. (2013). Potential of Solar Thermal Energy Utilization In Electrical Generation. *2nd International Conference on Energy Systems and Technologies,* 18 – 21 Feb., Cairo, Egypt.

Aldali, Y., Davison, B., Muneer, T., & Henderson, D. (2011). Modeling the behavior of a 50MW DSG plant for southern Libya based on the thermodynamic and thermophysical properties of water substance. *ASME* .134.2012.

Da Rocha, A. M. (2010). Analysis on Solar Retrofit in Combined Cycle Power Plants. Master thesis. *Fakultät für Maschinenwesen und Betriebswissenschaften*, Technische Universität Wien.

Eck, M., & Zarza, E. (2006). Saturated steam process with direct steam generating parabolic troughs. *Solar Energy, 80*, 1424-1433. http://dx.doi.org/10.1016/j.solener.2006.03.011

Eck, M., Zarza, E., Eickhoff, M., Rheinländer, J., & Valenzuela, L. (2003). Applied research concerning the direct steam generation in parabolic troughs. *Solar Energy, 74*, 341-351. http://dx.doi.org/10.1016/S0038-092X(03)00111-7

Elsaket, G. (2007). *Simulating the Integrated Solar Combined Cycle for Power Plants Application in Libya*. MSc Thesis, School of Engineering, Cranfield University.

El-Sayed, M. A. H. (2005). Solar supported steam production for power generation in Egypt. *Energy Policy, 33*(4), 1251-1259. http://dx.doi.org/10.1016/j.enpol.2003.11.021

Garcia, I. L., Luis, J. A., & Blanco, D. (2011). Performance model for parabolic trough solar thermal power plants with thermal storage: Comparison to operating plant data. *Solar Energy, 85*, 2443-2460. http://dx.doi.org/10.1016/j.solener.2011.07.002

Garcia-Barberena, J., Garcia, P., Sanchez, M., Blanco, M. J., Lasheras, C., Padros, A., & Arraiza, J. (2012). Analysis of the influence of operational strategies in plant performance using SimulCET, simulation software for parabolic trough power plants. *Solar Energy, 86*, 53-63. http://dx.doi.org/10.1016/j.solener.2011.09.018

Horn, M., Führing, H., & Rheinländer, J. (2004). Economic analysis of integrated solar combined cycle power plants. A sample case: The economic feasibility of an ISCCS power plant in Egypt. *Energy, 29*, 935-945. http://dx.doi.org/10.1016/S0360-5442(03)00198-1

Hosseini, R., Soltani, M., & Valizadeh, G. (2005). Technical and Economic Assessment of the Integrated Solar Combined Cycle Power Plants in Iran. *Renewable Energy, 30*, 1541-1555. http://dx.doi.org/10.1016/j.renene.2004.11.005

Kelly, B., Herrmann, U., & Hale, M. J. (2001). Optimization Studies for Integrated Solar Combined Cycle Systems. *Proceedings of Solar Forum, Solar Energy*: The Power to Choose April 21-25, Washington, DC.

Khaldi, F. (2011). Air bottoming cycle for hybrid solar-gas power plants. *Word Renewable Energy Congress*, 8-11 May, Linköping, Sweden.

Liu, H., & Jordon, R. (1960). The interrelationship and characteristic distribution of direct, diffuse and total solar radiation. *Solar Energy, 4*(3), 1-19. http://dx.doi.org/10.1016/0038-092X(60)90062-1

Montes, M. J., Abanades, A., Martınez-Val, J. M., & Valdes, M. (2009). Solar multiple optimization for a solar-only thermal power plant, using oil as heat transfer fluid in the parabolic trough collectors. *Solar Energy, 83*, 2165-2176. http://dx.doi.org/10.1016/j.solener.2009.08.010

Peterseim, J. H., White, S., Tadros, A., & Hellwig, U. (2012). Integrated Solar Combined Cycle Plants Using Solar Power Towers to Optimise Plant Performance. *SolarPACES Conference*, Marrakech, 11-14 September.

Popov, D. (2011). An Option for Solar Thermal Repowering of Fossil Fuel Fired Power Plants. *Solar Energy, 85*, 344-349. http://dx.doi.org/10.1016/j.solener.2010.11.017

Sukhatme, S. P. (2008). Principles of Thermal Collection and Storage. *Tata McGraw-Hill Publishing Co. Ltd*., New Delhi, India.

Tham, Y. W., Muneer, T., & Davison, B. (2010). Estimation of hourly averaged solar irradiation: evaluation of models. *Building services research and technology, 31*(1), 9-25. http://dx.doi.org/10.1177/0143624409350547

Torres, F. A., Ortega, E. S., García, A. S., & Martínez, R. F. (2012). Technical Feasibility Assessment of Integrated Solar Combined Cycle Power Plants in Ciudad Real (Spain) and Las Vegas (USA). *XVI Congreso Internacional de Ingeniería de Proyectos Valencia*, 11-13 de julio de 2012.

Valenzuela, L., Zarza, E., Berenguel, M., & Camacho, E. F. (2006). Control scheme for direct steam generation in parabolic troughs under recirculation operation mode. *Solar Energy, 80*, 1-17. http://dx.doi.org/10.1016/j.solener.2005.09.009

Wood, A. (2012). Solar Hybrid Solutions. *4th Saudi Solar Forum* 9th May.

Zarza, E., Valenzuela, L., Leon, J., Hennecke, K., Eck, M., Weyers, D., & Eickhoff, M. (2004). Direct Steam Generation in Parabolic Troughs: Final Results and Conclusions of the DISS Project. *Energy, 29*(5-6), 635-644. http://dx.doi.org/10.1016/S0360-5442(03)00172-5